

## Electronic structure of $p$ -type $\text{SrTiO}_3$ by photoemission spectroscopy

T. Higuchi and T. Tsukamoto

*Faculty of Science, Science University of Tokyo, 1-3 Kagurazaka, Shinjuku, Tokyo 162, Japan*

N. Sata and M. Ishigame

*Research Institute for Scientific Measurement, Tohoku University, 2-1-1 Katahira, Sendai, Miyagi 980, Japan*

Y. Tezuka and S. Shin

*Synchrotron Radiation Laboratory, Institute for Solid State Physics, University of Tokyo, 3-2-1 Midori-cho, Tanashi, Tokyo 188, Japan*

(Received 28 July 1997)

The electronic structure of  $p$ -type  $\text{SrTiO}_3$  has been studied by photoemission spectroscopy (PES). Comparing with the PES of  $n$ -type  $\text{SrTiO}_3$ , the Fermi level of  $p$  type is lower by about 0.7 eV and a prominent feature of Ti  $3d$  character within the band gap, which is formed in the  $n$ -type  $\text{SrTiO}_3$ , cannot be found in  $p$ -type  $\text{SrTiO}_3$ . It is suggested that the band structure of  $p$ -type  $\text{SrTiO}_3$  follows the rigid-band model. The resonant photoemission study shows that the Ti  $3d$  partial density of states in the valence band of  $p$ -type  $\text{SrTiO}_3$  is much larger than that of  $n$ -type  $\text{SrTiO}_3$ . Furthermore, it is also found that the satellite intensities of several core lines in  $p$ -type  $\text{SrTiO}_3$  are stronger than those in  $n$ -type  $\text{SrTiO}_3$ . These facts suggest that the hybridization effect between the Ti  $3d$  and O  $2p$  states becomes stronger in  $p$ -type  $\text{SrTiO}_3$ . [S0163-1829(98)03312-8]

### I. INTRODUCTION

Strontium titanate ( $\text{SrTiO}_3$ ) is one of the most typical perovskite-type compounds with a band gap of about 3.2 eV.<sup>1</sup> It is well known that the  $\text{SrTiO}_3$  crystal has  $n$ -type conductivity by doping cations such as  $\text{Nb}^{5+}$ ,  $\text{La}^{3+}$ , and  $\text{Y}^{3+}$  and it becomes a superconductor. The electronic structure of Nb-doped  $\text{SrTiO}_3$  has been reported in several photoemission spectroscopy studies.<sup>2,3</sup> In a simple ionic model, a titanium ion in  $\text{SrTiO}_3$  is tetravalent and has no  $3d$  electrons. Since there are no  $3d$  electrons nominally that bring appreciable correlation interactions, the electronic structure of  $\text{SrTiO}_3$  is possibly described by the energy-band picture. In fact, a lot of theoretical calculations of electronic band structures have also been performed on  $n$ -type  $\text{SrTiO}_3$ .<sup>4-6</sup> In  $\text{SrTiO}_3$ , the top of the valence band is mainly composed of O  $2p$  states and the bottom of the conduction band is formed by the Ti  $3d$  states. However, it is known that the orbital of  $3d$  electrons in titanium is strongly hybridized with those in oxygen. This leads to the situation in which nonvanishing  $3d$  electrons exist in the ground state. Thus, interesting properties in the photoemission spectra are found in the satellite structures of the light transition-metal compounds. Van der Laan<sup>7</sup> observed satellites in the Ti  $2p$  absorption spectra, and strong satellites were observed in the Ti  $2p$  photoemission spectra.<sup>3,8-13</sup> These satellites are considered to be caused by the charge-transfer (CT) -type satellites.

The  $\text{Sr}_{1-x}\text{La}_x\text{TiO}_3$  has been studied extensively by x-ray absorption and photoemission spectra so far. The  $3d$  state appears due to the La doping in the band gap below the Fermi level.<sup>14</sup> The small Fermi edge, which should be responsible for the superconductivity, was found.<sup>15</sup> The intensity of the  $3d$  state in the band gap becomes larger as the La concentration increases.<sup>14</sup> By O  $1s$  absorption,<sup>14</sup> the energy shift to the lower energy region was found and the intensity

at the absorption edge becomes larger as the La concentration increases.

Recently, it was found that  $\text{SrTiO}_3$  shows a hole conductivity as well as protonic conductivity when doped with Sc ions.<sup>16</sup> The protonic conductor is expected to be the hydrogen sensor or fuel cell because of its protonic conductivity at high temperature. The electrical conductivity shows a thermal activation-type behavior with activation energy of about 0.4 eV. It is suggested that proton migrates by hopping from site to site around the oxygen ion in this material.<sup>17,18</sup>

There have been a lot of studies about the application of this material; however, the electronic structure of  $p$ -type  $\text{SrTiO}_3$  has not been studied much. The electronic structure of  $p$ -type  $\text{SrTiO}_3$  has been studied by the absorption spectra of vacuum ultraviolet region.<sup>19</sup> The energy shift of the absorption edge due to acceptor doping was observed in  $p$  type and the band gap was found to increase by increasing the dopant concentration. It is suggested that holes are formed at the top of the valence band of  $p$ -type  $\text{SrTiO}_3$  due to acceptor doping. Thus, this shift is thought to be followed by the rigid-band model.

In this paper, the electronic structure of  $p$ -type  $\text{SrTiO}_3$  ( $\text{SrTi}_{0.98}\text{Sc}_{0.02}\text{O}_3$ ), in which acceptor ion ( $\text{Sc}^{3+}$ ) were introduced into  $\text{Tr}^{4+}$  ion site in  $\text{SrTiO}_3$ , has been studied by photoemission. It is unclear whether the valence-band structure of the  $p$ -type  $\text{SrTiO}_3$  may be characterized by the rigid-band model. As a reference material, the photoemission of the  $n$ -type  $\text{SrTiO}_3$  ( $\text{SrTi}_{0.98}\text{Nb}_{0.02}\text{O}_3$ ) was also measured.

### II. EXPERIMENT

The single crystal of  $p$ -type  $\text{SrTiO}_3$  was grown by the floating-zone method using Xe-arc imaging furnace. The hydrostatically pressed rod that consists of  $\text{SrTiO}_3$ ,  $\text{SrCO}_3$ , and

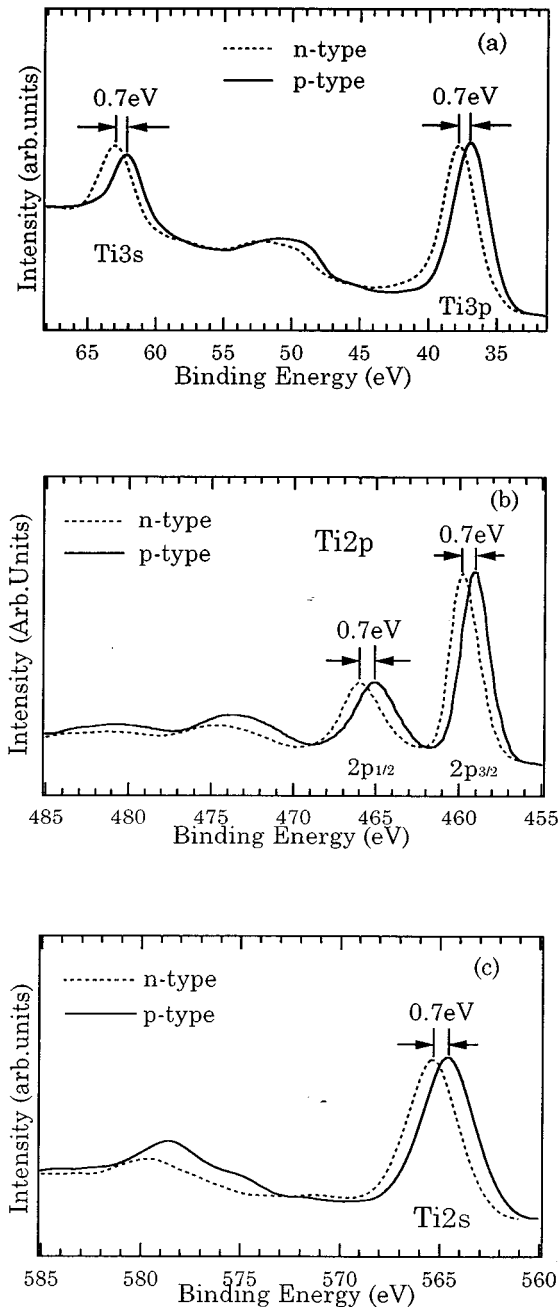


FIG. 1. Comparisons of several core lines in the photoemission spectra of *n*- and *p*-type SrTiO<sub>3</sub>. The ordinates are normalized by the intensities of the main peaks. Solid and dashed lines indicate the *p*- and *n*-type SrTiO<sub>3</sub>.

Sc<sub>2</sub>O<sub>3</sub> powder was used. The crystals were examined using x-ray diffraction.

The single crystals of *n*-type SrTiO<sub>3</sub>, which were grown by the Czochralski method, were obtained from Earth Jewelry Co. Ltd.

The photoemission spectra were measured at BL-2 of SOR-RING of the Synchrotron Radiation Laboratory, Institute for Solid State Physics (ISSP), University of Tokyo. Synchrotron radiation was monochromatized using a grazing-incidence spherical grating monochromator. The kinetic energy of the photoelectron was measured with a double-pass cylindrical mirror analyzer. The total resolution

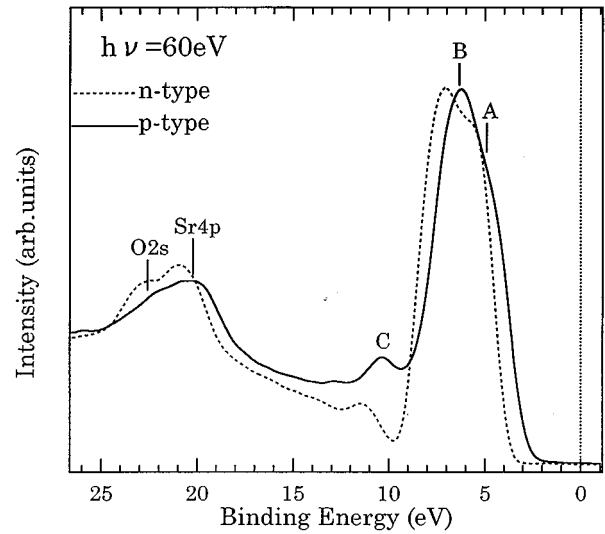


FIG. 2. Comparison of EDC's between *n*- and *p*-type SrTiO<sub>3</sub> in the valence-band energy region.

of the experimental system was about 0.3 eV. The x-ray photoemission spectroscopy (XPS) spectra were also measured by the Mg *K* α line (1253.6 eV) as the excitation light source. The photoelectron was measured by the electrostatic hemispherical spectrometer whose radius is 100 mm. The total-energy resolution was about 1.0 eV.

The samples were scraped *in situ* with a diamond file in a vacuum of  $3.0 \times 10^{-10}$  Torr in order to obtain the clean surface. Since the *p*-type SrTiO<sub>3</sub> has little conductivity at room temperature, the sample is charged. On the other hand, the sample has a finite conductivity at high temperature. Thus, the measurement was carried out at 393 K to avoid the charging. The position of the Fermi level has been determined by measuring the Fermi edge of Au.

### III. RESULTS AND DISCUSSION

Figure 1 shows the comparison of several energy distributions curves (EDC's) between *n*-type SrTi<sub>1-x</sub>Nb<sub>x</sub>O<sub>3</sub> and *p*-type SrTi<sub>1-x</sub>Sc<sub>x</sub>O<sub>3</sub>. The figure shows the spectra of Ti 3*s*, 3*p*, 2*p*, and 2*s* core regions measured at  $h\nu = 1253.6$  eV, respectively. Solid and dotted lines show the comparison of EDC's of *n*- and *p*-type SrTiO<sub>3</sub>, respectively. The intensities of these spectra are normalized by the peak intensities of the main lines. Satellite structures having energy separations of about 13.6 eV are found in all these core lines. The binding energy ( $E_B$ ) of Ti 3*p* core levels in *n* type is 37.6 eV, and that in *p* type is 36.9 eV. The Ti 3*s*, 2*p*, and 2*s* core lines are located at 62.4, 459, and 39.4 eV in *n* type, and at 61.7, 458.3, and 564.7 eV in *p* type. That is, every Ti line undergoes a core-level shift to lower binding energy by about 0.7 eV in *p*-type SrTi<sub>1-x</sub>Sc<sub>x</sub>O<sub>3</sub>. This fact means the Fermi level becomes lower in *p*-type SrTiO<sub>3</sub>.

Figure 2 shows the comparison of the EDC spectra in the valence-band region between the *p*- and the *n*-type samples. The valence-band spectra have two features A and B, which mainly consist of O 2*p* states mixed with Ti 3*d* states. It is known that feature A corresponds to the nonbonding state and that feature B corresponds to the bonding state that is

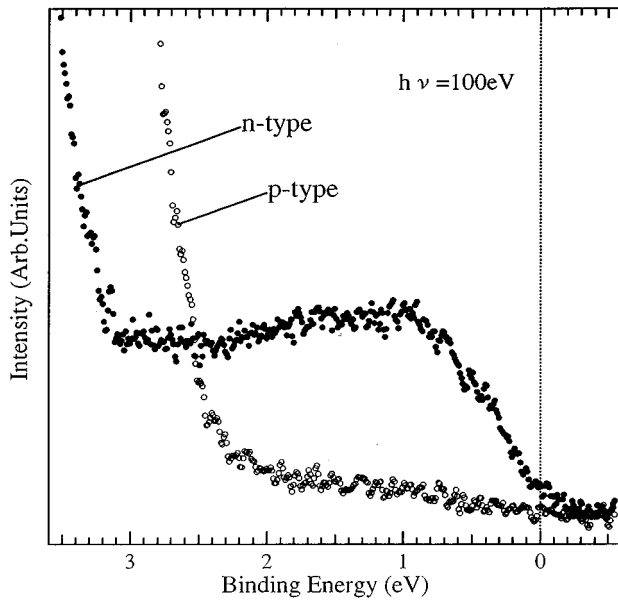


FIG. 3. Photoemission spectra near the Fermi level on an expanded scale for *n*- and *p*-type SrTiO<sub>3</sub>. The donor band exists only in the band gap of the *n*-type SrTiO<sub>3</sub>.

well mixed with the Ti 3*d* states. Feature *C* is considered to be the defect of oxygen at the surface.<sup>2</sup> It has been reported by Betrel<sup>20</sup> that the doublet structures at around 20 eV are the O 2*s* and Sr 4*p* lines. The intensities of both *n*- and *p*-type spectra are normalized by the peak intensities of Sr 4*p*. The peak position of *A* and *B* are different in the spectra of *n* and *p* type. Features *A* and *B* are observed at 4.7 and 6.7 eV in *n* type, while at 4.0 and 6.0 eV in *p* type. Therefore, the position of the valence-band top is shifted to lower binding energy by about 0.7 eV in *p*-type SrTiO<sub>3</sub>. This fact seems to be consistent with the energy shifts in Ti core lines. This shift of the Fermi level indicates the effect of the doping on the rigid-band model.

In *n*-type material, the  $E_F$  is located just at the bottom of the conduction band because the band gap is about 3.2 eV and the energy between the top of the valence band and the  $E_F$  is about 3.2 eV in Fig. 2. In the case of *p*-type material, the top of the valence band is found to be located at about 2.6 eV below the  $E_F$ , while the band gap of *p*-type SrTiO<sub>3</sub> was obtained at 3.54 eV.<sup>19</sup> This fact indicates that the Fermi level is located close to the conduction band in the band gap. If the electronic structure obeys the rigid-band model exactly, the position of the  $E_F$  of the *p* type one would be located below the half of the band gap. Thus, the energy shift observed in this measurement seems to be small. This fact may reflect the band bending effect at the surface. It is known that the bands at the surfaces of ordinary semiconductors bend upward or downward in the *n*- or *p*-type samples, respectively.<sup>21</sup> This effect may depend on the space charge trapped by the surface state. The surface state has been studied well in *n*-type semiconductors, while it has not been studied well in *p*-type semiconductors. It is known that Sc-doped SrTiO<sub>3</sub> has a lot of oxygen defects. It is believed that the extra charge is trapped by defects at the surface. Another possible origin of the apparent discrepancy is that the photoemission is a spatially localized phenomenon,

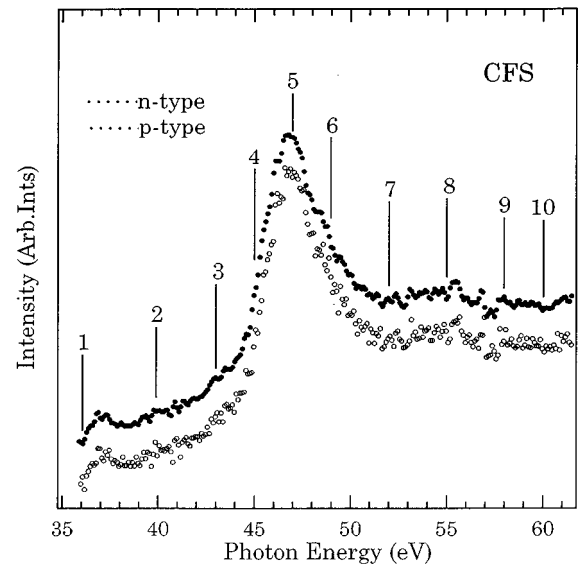


FIG. 4. The CFS spectra of *n*- and *p*-type SrTiO<sub>3</sub> corresponding to the Ti 3*p* absorption spectra. Closed and open circles indicate *p*- and *n*-type SrTiO<sub>3</sub>. The numbers indicate the photon energies, where the resonant-photoemission spectra were measured.

whereas the  $E_F$  observed in conductivity measurement is macroscopic. Here, the location of the  $E_F$  cannot be explained quantitatively. However, the difference of the  $E_F$  between *n* and *p* type is consistent with the rigid-band model.

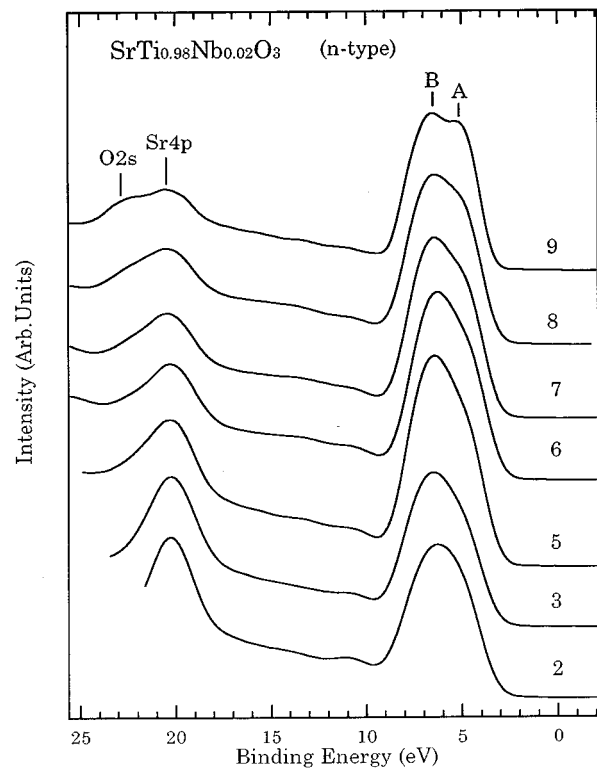


FIG. 5. Valence-band spectra of *n*-type SrTiO<sub>3</sub> excited at various photon energies numbered in Fig. 4. Labels *A* and *B* indicate the nonbonding and bonding band between the O 2*p* and Ti 3*d* states.

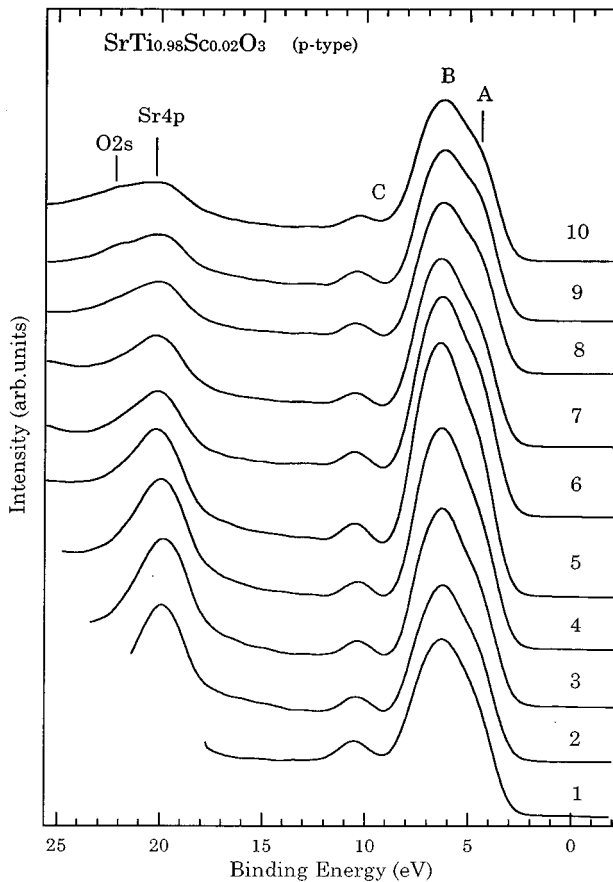


FIG. 6. Valence-band spectra of *p*-type SrTiO<sub>3</sub> excited at various photon energies numbered in Fig. 4.

Figure 3 shows the detailed photoemission spectra in the band-gap energy region below the Fermi level, where the open and closed circles indicate the EDC spectra of *p*- and *n*-type SrTiO<sub>3</sub>. A prominent feature that has a *3d* character was found at around  $E_B = 1$  eV in the band gap. The feature mainly originates from the donor band formed by doping.<sup>14</sup> There is a Fermi edge for *n*-type SrTiO<sub>3</sub>, though the intensity at  $E_F$  is very little. However, there is no structure in the band gap below the Fermi level in *p*-type SrTiO<sub>3</sub>. This fact is consistent with the rigid-band model, which suggests that there is a structure in the band gap above the Fermi level in the case of *p*-type SrTiO<sub>3</sub>.

A *3d* character band has been found in the band gap of La-doped *n*-type SrTiO<sub>3</sub>.<sup>14</sup> There is the difference of binding energy from the donor band, which is considered to be 1.5 eV in La doped, and  $\sim 0.8$  eV in Nb doped. The origin of the formation of the gap state has not been clear. In *n*-type La-doped SrTiO<sub>3</sub>, Fujimori *et al.*<sup>14</sup> interpreted that the density of states (DOS) observed in the band gap is not simply a donor band. Impurity potential due to the La<sup>3+</sup> ions substituting Sr<sup>2+</sup> produces donor levels, but the binding energy of such a donor level would be orders of magnitude too small to account for the  $\sim 1.5$  eV peak. And, the long-range Coulomb interaction combined with potential disorder might cause a pseudogap in metallic systems,<sup>22</sup> since it is known to produce a Coulomb gap in insulators.<sup>23</sup> Such an effect, however, depends on the mean distance between doped electrons and hence should diminish with decreasing *X*. In this study, one

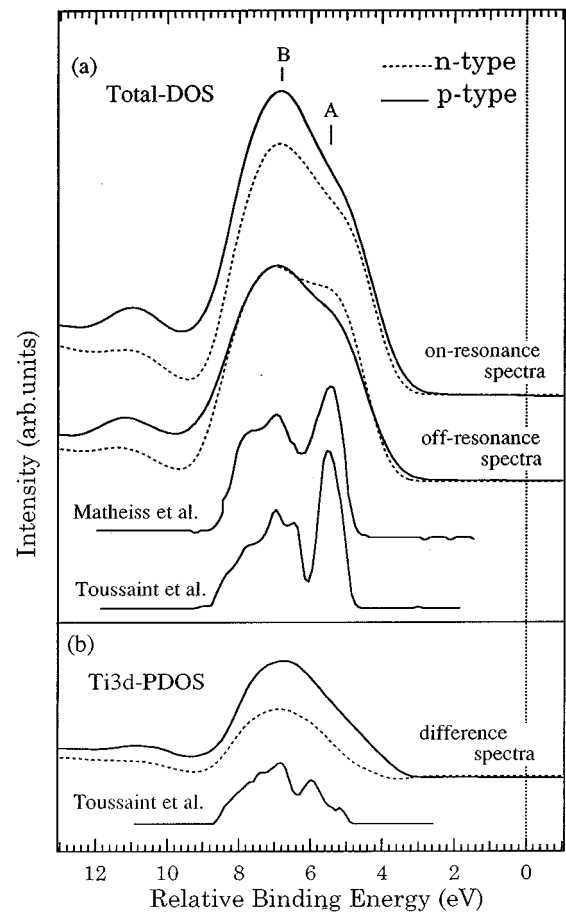


FIG. 7. (a) Comparison between the on- and off-resonance spectra for *n*- and *p*-type SrTiO<sub>3</sub>. Shown are total DOS curves calculated by Matheiss (Ref. 4) and Toussaint, Selme, and Pecheur (Ref. 24). (b) Difference spectra from on- to off-resonance spectra and Ti *3d* PDOS curve calculated by Toussaint, Selme, and Pecheur. Solid and broken lines show *p*- and *n*-type SrTiO<sub>3</sub>.

can find there is no structure in the band gap in the *p*-type SrTiO<sub>3</sub>. This fact supports at least that this band comes from the donor bands, though there are a lot of questions regarding the origin of the formation of this band.

Figure 4 shows the constant final state (CFS) spectra of *p*- and *n*-type SrTiO<sub>3</sub> measured at the kinetic energy, where the secondary electron has a maximum intensity. These spectra are approximately regarded as the absorption spectra of Ti *3p*  $\rightarrow$  Ti *3d*. The vertical bars, which are numbered from 1 to 10, indicate the selected photon energies for the resonant-photoemission measurements.

Figures 5 and 6 show the valence-band EDC's of *n*- and *p*-type SrTiO<sub>3</sub> measured at various photon energies numbered in Fig. 4. Labels A and B indicate the nonbonding and bonding bands of the O *2p* and Ti *3d* states. The bonding peak of the valence band is enhanced around the photon energy 47 eV (label 5). The Ti *3p*  $\rightarrow$  *3d* resonance enhancement of bonding peak in *p* type is larger than that in *n* type. The intensity of the Sr *4p* peak at about 23.2 eV becomes strong at lower excitation energies. This is obviously due to the excitation-energy dependence of the ionization cross section of the Sr *4p* electron.<sup>3</sup> Since the Sr *4p* line is observed

strongly, the O  $2s$  line is distinguished as a shoulder on the tail of the Sr  $4p$  line.

Figure 7(a) shows off-resonance spectra of the valence band of  $n$ - and  $p$ -type SrTiO<sub>3</sub>. The excitation energy for the spectra is 60 eV. The binding energy of the  $p$ -type SrTiO<sub>3</sub> is shifted to higher binding energy by 0.7 eV in order to compare the line shape with that of the  $n$ -type one. Two energy-band DOS curves shown under off-resonance spectra obtained by several authors, Mattheiss<sup>4</sup> and Toussaint, Selme, and Pecheur,<sup>24</sup> are also exhibited. Each of the DOS curves are obtained by convoluting the original DOS with Gaussian broadening functions with widths of 0.5 eV. Mattheiss calculated his DOS curves using the augmented plane wave and Slater-Coster linear combination of atomic orbitals interpolation method.<sup>4</sup> Toussaint *et al.* calculated DOS curves using the tight-binding method, together with a Green's function.<sup>24</sup> The off-resonance spectra are in good accordance with the band calculation by Mattheiss<sup>4</sup> and Toussaint, Selme, and Pecheur.<sup>24</sup> In two band calculations, the valence band has two peaks. The photoemissions spectra also show the two peaks, A and B (nonbonding and bonding peaks), although the intensity of peak A is lower than that of peak B in the photoemission spectra. One can find that the intensity of the nonbonding peak of the  $p$  type is lower than that of the  $n$  type. Furthermore, the Ti  $3d$  components in both bonding and nonbonding bands are resonantly enhanced by the Ti  $3p \rightarrow 3d$  excitation in the on-resonance spectra. The effect strongly appears in  $p$ -type SrTiO<sub>3</sub>.

Figure 7(b) shows the difference spectra from on-resonance to off-resonance spectra.

It is known that the difference spectra by the resonant photoemission correspond to the  $3d$  components in the valence band. One can find that the difference spectrum of  $p$ -type SrTiO<sub>3</sub> has a stronger intensity than  $n$ -type material. This fact shows that the  $3d$  component of  $p$ -type SrTiO<sub>3</sub> is more than that of  $n$ -type SrTiO<sub>3</sub>. Thus, one can know that the hybridization between O  $2p$  and Ti  $3d$  increases in  $p$ -type SrTiO<sub>3</sub>. In fact, the difference spectra are in good agreement with the calculated Ti  $3d$  partial density of states (PDOS) by Toussaint, Selme, and Pecheur,<sup>24</sup> which is shown under two difference spectra.

Figure 8 shows the XPS and ultraviolet photoemission spectroscopy spectra in several core levels. The abscissa represents the relative binding energy, the zero of which is located at the main peak. The core levels are indicated on the left-hand sides of the spectra. The vertical bars in EDC spectra indicate the location of the charge-transfer satellites. The core-level XPS spectra of SrTiO<sub>3</sub> have been already reported by Kim and Winograd *et al.*<sup>11</sup> and Tezuka *et al.*<sup>3</sup> The present results are consistent with their results. It is known that these satellites are closely related to the hybridization effect between Ti  $3d$  and O  $2p$  in SrTiO<sub>3</sub>.

It is recognized that the charge-transfer satellites are observed in every spectrum about 13.6 eV from the main line in both  $n$ - and  $p$ -type SrTiO<sub>3</sub>. Furthermore, it is found that the intensities of the satellites in  $p$  type are stronger than those in  $n$ -type SrTiO<sub>3</sub>. The relative intensities of the satellite to the main structures are almost 10–15 % for the  $2p$ ,  $3s$ , and  $3p$  and about 30% for the  $2s$  structure in  $n$ -type SrTiO<sub>3</sub>.<sup>3</sup> On the other hand, the relative intensities of those are almost 15–20 % for the  $2p$ ,  $3s$ , and  $3p$ , and about 35%

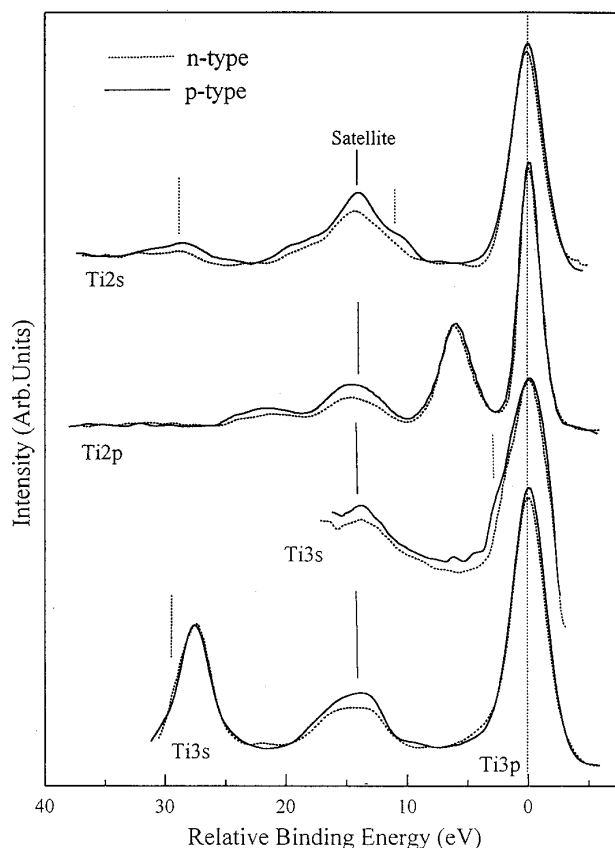


FIG. 8. Core-photoemission spectra of  $n$ - and  $p$ -type SrTiO<sub>3</sub>. The abscissa is the relative binding energy from the main peak. Solid and broken lines show  $p$ - and  $n$ -type SrTiO<sub>3</sub>. Vertical bars show the satellites.

for the  $2s$  structure in  $p$ -type SrTiO<sub>3</sub>.

These differences in the satellite intensities are not clear at present, because satellite intensity is related to several parameters; hybridization energy  $V$ , charge-transfer energy  $\Delta$ , and core hole potential  $V_{dc}$ . Here, there is a problem in the energy separation between the main line and satellite line. They are about 13.6 eV in both spectra. If only the hybridization of the Ti  $3d$  and O  $2p$  states becomes stronger in the  $p$ -type one, the energy position of the satellite in  $p$  type would be larger than that in  $n$  type. Recently, Okada and Kotani<sup>25</sup> calculated the charge-transfer (CT) satellite in the Ti  $2p$  core region of Ti compounds. The energy separation of the satellite structure is well reproduced by calculation, where the energy separation is mainly due to the large hybridization effect  $V$  and the CT energy ( $\Delta$ ). It is roughly determined to be  $\sqrt{\Delta^2 + 4V_{\text{eff}}^2}$ , where the  $V_{\text{eff}}$  is  $\sqrt{6V(t_{2g})^2 + 4V(e_g)^2}$ , and  $V(t_{2g})$  and  $V(e_g)$  are the hybridization energies of  $t_{2g}$  and  $e_g$  states. Since the energy separation does not change much, the other parameters are changed between  $n$ - and  $p$ -type SrTiO<sub>3</sub>. These changes of the parameters may be due to the slight change of the lattice constant and the screening effect by the free carriers in  $n$ -type SrTiO<sub>3</sub>.

The vertical dashed lines show the plasmon satellites. The dashed line in the Ti  $3s$  is due to the plasmon of Ti  $3p$  core line. A plasmon satellite is observed at about 28 eV. Frandon, Brousseau, and Pradal<sup>26</sup> observed the plasmon peak at 26 eV by means of electron-energy-loss study. Sen, Riga,

and Verbist<sup>10</sup> also observed the satellites at 26 eV in the Ti 2*s* and Ti 2*p* spectra. In this study, the plasmon satellite is observed in the Ti 2*s* and Ti 3*p* spectra, though it is not observed clearly in the Ti 2*p* and Ti 3*s* spectra.

In the Ti 2*s* spectrum, the charge-transfer satellite is formed at about 10 eV from the main peak. These structures may be nonbonding-type charge-transfer satellites, which are found in on-resonance spectra of early transition-metal compounds, such as ScF<sub>3</sub> (Ref. 27) and TiO<sub>2</sub>.<sup>3,8-13</sup> This nonbonding satellite becomes stronger in *p*-type SrTiO<sub>3</sub>, which is also consistent with the larger hybridization in *p*-type SrTiO<sub>3</sub>.

#### IV. CONCLUSION

We measured photoemission spectra on *p*-type SrTiO<sub>3</sub> using synchrotron radiation, and compared the results with those of the Nb-doped *n*-type SrTiO<sub>3</sub>. The valence-band and Ti core levels are shifted by about 0.7 eV. The donor band is found in the band gap below Fermi level in the *n*-type SrTiO<sub>3</sub>, but cannot be found in the *p*-type one. These results can be understood by the rigid-band model. In the resonant-photoemission study, the Ti 3*d* state in the valence band is much stronger in *p*-type SrTiO<sub>3</sub>. It is concluded that the hybridization with O 2*p* and Ti 3*d* is increased in *p*-type SrTiO<sub>3</sub>.

- 
- <sup>1</sup>M. Cardona, Phys. Rev. A **651**, 140 (1965).  
<sup>2</sup>B. Reihl, J. G. Bednorz, K. A. Müller, Y. Jugnet, G. Landgren, and J. F. Morar, Phys. Rev. B **30**, 803 (1984).  
<sup>3</sup>Y. Tezuka, S. Shin, T. Ishii, T. Ejima, S. Suzuki, and S. Sato, J. Phys. Soc. Jpn. **63**, 347 (1994).  
<sup>4</sup>L. F. Mattheiss, Phys. Rev. B **6**, 4718 (1972).  
<sup>5</sup>T. F. Soules, E. J. Kelly, and D. M. Vaught, Phys. Rev. B **6**, 1519 (1972).  
<sup>6</sup>P. Pertosa and F. M. Michel-Calendini, Phys. Rev. B **17**, 2011 (1978).  
<sup>7</sup>G. van der Laan, Phys. Rev. B **41**, 12 366 (1990).  
<sup>8</sup>B. Wallbank, C. E. Johnson, and I. G. Main, J. Phys. C **6**, L493 (1973).  
<sup>9</sup>I. Ikemoto, K. Ishii, H. Kuroda, and J. M. Thomas, Chem. Phys. Lett. **28**, 55 (1974).  
<sup>10</sup>S. K. Sen, J. Riga, and J. Verbist, Chem. Phys. Lett. **39**, 560 (1976).  
<sup>11</sup>K. S. Kim and N. Winograd, Chem. Phys. Lett. **31**, 312 (1975).  
<sup>12</sup>T. Uozumi, K. Okada, A. Kotani, R. Zimmermann, P. Steiner, S. Hüfner, Y. Tezuka, and S. Shin, J. Electron Spectrosc. Relat. Phenom. **83**, 9 (1997).  
<sup>13</sup>S. P. Kowalczyk, F. R. McFeely, L. Ley, V. T. Grimsyn, and D. A. Shirley, Solid State Commun. **23**, 161 (1977).  
<sup>14</sup>A. Fujimori, I. Hase, M. Nakamura, H. Namatame, Y. Fujishima, and Y. Tokura, Phys. Rev. B **46**, 9841 (1992).  
<sup>15</sup>V. E. Henrich and R. L. Kurtz, J. Vac. Sci. Technol. **18**, 416 (1981).  
<sup>16</sup>H. Iwahara, T. Esaka, H. Uchida, and N. Maeda, Solid State Ionics **3/4**, 359 (1981); N. Sata, M. Ishigame, and S. Shin, Phys. Rev. B **54**, 15 795 (1996).  
<sup>17</sup>S. Shin, H. H. Huang, M. Ishigame, and H. Iwahara, Solid State Ionics **40/41**, 910 (1990).  
<sup>18</sup>H. H. Huang, M. Ishigame, and S. Shin, Solid State Ionics **47**, 251 (1991).  
<sup>19</sup>N. Sata, M. Ishigame, and S. Shin, Solid State Ionics **86**, 629 (1996).  
<sup>20</sup>E. Betrel, Phys. Rev. B **27**, 1939 (1983).  
<sup>21</sup>S. Shin, A. Agui, M. Fujisawa, Y. Tezuka, T. Ishii, Y. Minagawa, Y. Suda, A. Ebina, O. Mishima, and K. Era, Phys. Rev. B **52**, 11 853 (1995).  
<sup>22</sup>A. Fujimori, K. Kawasaki, and N. Tsuda, Phys. Rev. B **38**, 7789 (1988).  
<sup>23</sup>J. H. Davis and R. L. Kurtz, J. Vac. Sci. Technol. **18**, 416 (1981).  
<sup>24</sup>G. Toussaint, M. O. Selme, and P. Pecher, Phys. Rev. B **36**, 6135 (1987).  
<sup>25</sup>K. Okada and A. Kotani, Spectrosc. Relat. Phenom. **62**, 131 (1993).  
<sup>26</sup>J. Frandon, B. Brousseau, and F. Pradal, J. Phys. (France) **39**, 839 (1978).  
<sup>27</sup>M. Umeda, Y. Tezuka, S. Shin, and A. Yagishita, Phys. Rev. B **53**, 1783 (1996).